23rd ABCM International Congress of Mechanical Engineering
December 6-11, 2015, Rio de Janeiro, RJ, Brazil

EXPERIMENTAL AND NUMERICAL MODELING OF HEAT CONDUCTION DURING FREEZING OF FOODS WITH STEEP VARIATIONS IN PROPERTIES

Fernando Zigunov
Flávia Zinani
Mechanical Engineering Graduate Program, Universidade do Vale do Rio do Sinos – UNISINOS – Av. Unisinos, 950 – Cristo Rei, São Leopoldo, RS, Brazil
fzigunov@gmail.com
fzinani@unisinos.br

Abstract. *This paper aims to evaluate the physical and numerical modeling of the freezing process of foods, whose thermophysical properties experience sudden variations during phase change. The finite differences method has been used to approximate the solution of the one-dimensional transient heat conduction problem in simple geometries (flat plate, infinite cylinder and sphere) with variable thermophysical properties and subjected to heat convection. The physical properties were modeled as dependent on food composition, temperature and phase. A pilot-scale freezing tunnel was developed to provide experimental data to validate the mathematical and numerical modeling. Several foods, shapes and convection coefficients have been tested, such as sausages, potatoes and cheese. Among thermophysical properties, the apparent specific heat experienced the greatest variations during freezing. The experiments showed that mass transfer (moisture evaporation) plays an important role on food freezing, and therefore a heat transfer numerical model is not enough to predict experimental results. As a solution, mass transfer was included in the numerical model so that it was able to predict experimental results with enough accuracy, and therefore it might be considered adequate to extrapolate this method to be used on more complex problems.*

Keywords: *Food freezing, transient heat conduction, finite differences, models for food thermal properties*

1. INTRODUCTION

Food freezing as a conservation process plays an important role in the global food industry. Even though it is so widely used, the complexity involved in the process makes it very difficult for one to forecast the food freezing times accurately. Nevertheless, the time of freezing is perhaps the most important variable to know before building a food freezing unit. In continuous freezing processes, usually performed in spiral or carton freezers, the size of the freezing equipment is proportional to the freezing time. Therefore, underestimating freezing time can lead to insufficient production capability of the equipment, whereas overestimating it may result in unnecessary costs in building materials, physical space and energy.

In this context, this paper's objective is to develop a numerical methodology to estimate food freezing times.

A major issue when dealing with modeling of food processes is the determination of food thermophysical properties, which are not only dependent on temperature and composition but on molecular microstructure itself. In processes in which there is phase change, the problems get more complex, because foods do not present a freezing point but a threshold temperature at which freezing begins. At this point, thermophysical properties experiment steep changes. Choi and Okos (1986) (*apud* ASHRAE, 2007) have modeled these changes, developing models for food properties as functions of temperature and composition. Their models are indicated by ASHRAE (2007) to be used in projects of freezing systems. As the use of realistic models for thermophysical properties is a key point to achieve reliable solutions, the use of analytical methods to determine freezing times is highly impaired. The usual method to determine freezing times is the use of empirical correlations, such as those of Plank (Stoeker, 2004) and Pham (1984).

In the present work, a numerical model to simulate heat conduction during food freezing was developed. It is based on the finite differences method, which employs the equations of Choi and Okos (1986) to model thermophysical properties. An experimental test bench, a pilot scale freezing tunnel, was also built in order to validate numerical results and elucidate some issues about the physics such processes. The numerical model was designed to solve one-dimensional transient conduction problems, therefore, it can only be applied to geometries that have one-dimensional temperature profiles: thin slab, long cylinder and sphere. Even though these geometries might be uncommon in carton freezers, they are frequently found in spiral and IQF freezers, such as hamburgers, meatballs, sausages, fish fillets, etc.

2. NUMERICAL MODEL

2.1 Transient heat conduction

A simple approach to solve the transient heat conduction problem is described in several books, such as Chapra & Canale (2010) did. The solutions described often oversimplify the problem to make it mathematically feasible to solve to an exact solution or to simplify the numerical calculations. Unfortunately, they are insufficient to solve for a problem where the product goes through a phase change, specially in the case of foods, where the properties experience a sudden variation. Therefore, some modifications are needed to make the numerical method adequate to solve this kind of problem.

It begins with the complete solution to the Fourier equation, already simplified to one dimensional conduction in the three solids that experience a one-dimensional temperature profile when subjected to constant surface conditions, as given by Incropera & DeWitt (2006):

$$\frac{1}{x^m}\cdot\frac{\partial}{\partial x}\cdot\left(kx^m\frac{\partial T}{\partial x}\right)=\rho\cdot c_p\cdot\frac{\partial T}{\partial t}\begin{cases}m=0\rightarrow Thin\ Slab\\ m=1\rightarrow Long\ Cylinder\\ m=2\rightarrow Sphere\end{cases} \tag{1}$$

where x is the spatial coordinate, k is the thermal conductivity of the solid, ρ is the specific mass of the solid, c_p is the specific heat of the solid, T is the temperature and t is the temporal coordinate.

Applying the outer partial derivative in Eq. 1 on the left side and dividing both sides by k, it is obtained:

$$\frac{1}{k\cdot x^m}\cdot\frac{\partial(kx^m)}{\partial x}\cdot\frac{\partial T}{\partial x}+\frac{\partial^2 T}{\partial x^2}=\frac{1}{\alpha}\cdot\frac{\partial T}{\partial t} \tag{2}$$

where α is the thermal diffusivity of the solid. Equation 2 is still hard to solve numerically because the term k is assumed to be dependent of the temperature. Since it depends on T and T depends on x, the partial derivative of kx^m in relation with x is hard to calculate. It was found that, with few iterations, the term $\varkappa$, shown in Eq. 3 can be assumed to be constant in order to calculate the temperature profile:

$$\varkappa=\frac{1}{k\cdot x^m}\cdot\frac{\partial(kx^m)}{\partial x} \tag{3}$$

So, the simplified version of Eq. 2 can be written as shown below, and it can be seen that it is similar to the most simplified version of the heat conduction equation, differing only by the presence of its first term. In fact, it has been found that the term $\varkappa$ has a large value and cannot be disregarded.

$$\varkappa\cdot\frac{\partial T}{\partial x}+\frac{\partial^2 T}{\partial x^2}=\frac{1}{\alpha}\cdot\frac{\partial T}{\partial t} \tag{4}$$

Using the Crank-Nicolson method to solve a computational 2D grid where T_i^l is the temperature on the spatial coordinate i and temporal coordinate l, it is relatively easy to solve Eq. 4 to the expression shown below:

$$\begin{gathered}T_{i+1}^{l+1}\cdot\lambda\cdot(2+\varkappa\cdot\Delta x)+T_i^{l+1}\cdot 4(-1-\lambda)+T_{i-1}^{l+1}\cdot\lambda\cdot(2-\varkappa\cdot\Delta x)=\cdots\\ \cdots T_{i+1}^{l}\cdot\lambda\cdot(-2-\varkappa\cdot\Delta x)+T_i^{l}\cdot 4(-1+\lambda)+T_{i-1}^{l}\cdot\lambda\cdot(-2+\varkappa\cdot\Delta x)\end{gathered} \tag{5}$$

where $\lambda=(\alpha\cdot\Delta t)/(\Delta x)^2$ is a dimensionless term defined by Chapra & Canale (2010) to establish a criteria for convergence in the explicit method. The left-hand temperature terms on Eq. 5 are all unknown, since the next timestep is to be calculated. All the right-hand terms are known. This equation has to be solved for all the terms in the spatial axis, and therefore a tridiagonal system of equations emerges. The system is best described in the matricial form, as shown in Eq. 6:

$$\begin{bmatrix} BC_{00} & BC_{10} & 0 & \cdots & 0 & 0 & 0 \\ A_{01} & A_{11} & A_{21} & \cdots & 0 & 0 & 0 \\ 0 & A_{12} & A_{22} & \cdots & 0 & 0 & 0 \\ \vdots & \vdots & \vdots & \ddots & \vdots & \vdots & \vdots \\ 0 & 0 & 0 & \cdots & A_{n-2,n-2} & A_{n-1,n-2} & 0 \\ 0 & 0 & 0 & \cdots & A_{n-2,n-1} & A_{n-1,n-1} & A_{n-1,n} \\ 0 & 0 & 0 & \cdots & 0 & BC_{n-1,n} & BC_{n,n} \end{bmatrix} \begin{bmatrix} T_0^{l+1} \\ T_1^{l+1} \\ T_2^{l+1} \\ \vdots \\ T_{n-2}^{l+1} \\ T_{n-1}^{l+1} \\ T_n^{l+1} \end{bmatrix} = \begin{bmatrix} C_0 \\ C_1 \\ C_2 \\ \vdots \\ C_{n-2} \\ C_{n-1} \\ C_n \end{bmatrix} \tag{6}$$

The terms inside the matrices can be written as:

$$A_{i-1,i} = \lambda \cdot (2 - \varkappa \cdot \Delta x) \tag{7}$$
$$A_{i,i} = 4(-1 - \lambda) \tag{8}$$
$$A_{i+1,i} = \lambda \cdot (2 + \varkappa \cdot \Delta x) \tag{9}$$
$$C_i = T_{i+1}^l \cdot \lambda \cdot (-2 - \varkappa \cdot \Delta x) + T_i^l \cdot 4(-1 + \lambda) + T_{i-1}^l \cdot \lambda \cdot (-2 + \varkappa \cdot \Delta x) \tag{10}$$

The terms BC are the boundary conditions, which are described in section 2.3.

2.2 Convection coefficients and mass transfer

Since the geometries used experimentally were simple, classical correlations, such as the ones given by Eqs. 11 to 14, were used to determine the convection coefficient (Incropera & DeWitt, 2006).

$$\overline{Nu_L} = 0{,}664 \cdot {Re_L}^{1/2} \cdot Pr^{1/3}\ [Laminar\ Plate] \tag{11}$$
$$\overline{Nu_L} = \left(0{,}037 \cdot {Re_L}^{4/5} - 871\right) \cdot Pr^{1/3}\ [Turbulent\ Plate] \tag{12}$$
$$\overline{Nu_D} = C \cdot {Re_D}^{m} \cdot Pr^{1/3}\ [Cylinder] \tag{13}$$
$$\overline{Nu_D} = 2 + \left(0{,}4 \cdot {Re_D}^{1/2} + 0{,}06 \cdot {Re_D}^{2/3}\right) \cdot Pr^{0{,}4} \left(\frac{\mu}{\mu_s}\right)^{1/4}\ [Sphere] \tag{14}$$

It was found experimentally that the wet surface of the product had an important influence on the temperature profile and therefore on the freezing time. Therefore, the mass transfer had also to be included on the convection model. This was accomplished by using the enthalpy potential (Stoecker & Jones, 1983), which simplifies greatly the mass transfer calculations. Equation 15 defines the heat flux provided by both sensible and latent heat transfer through the wet surface:

$$q'' = h \frac{\left(H_{air,s} - H_{air,\infty}\right)}{c_{p,m}} \tag{15}$$

where q'' is the total heat flux through the wet surface, h is the heat convection coefficient, calculated in the conventional way, $H_{air,s}$ is the enthalpy of the air, given the surface temperature and humidity, $H_{air,\infty}$ is the enthalpy of the surrounding air and $c_{p,m}$ is the moist air specific heat, which can be calculated as

$$c_{p,m} = c_{p,air} + W \cdot c_{p,w} \tag{16}$$

where $c_{p,air}$ is the specific heat of the dry air, W is the absolute humidity and $c_{p,w}$ is the specific heat of the water vapor, given the temperature of the air.

With these relationships, the total heat flux could be calculated and used as a boundary condition in the model.

2.3 Boundary conditions

Even though there are different models for boundary conditions (namely Dirichlet, Neumann and Robin are the most widely used), only the Neumann boundary model has been used in this work. Although the convection coefficient was given, the mass transfer calculations aforementioned resulted in a given value of q'', instead of h.

As mentioned by Ozisik (1994), the Neumann boundary condition can be written as a known value of the partial derivative of the temperature in relation with the distance, on the boundary:

$$\frac{\partial T^{l+1}}{\partial x_0} = constant \tag{17}$$

Using the Fourier equation and developing the algebra, it can be proved that:

$$T_0^{l+1} - T_1^{l+1} = -q'' \cdot \frac{\Delta x}{k} \tag{18}$$

2.4 Food properties

The ASHRAE Handbooks (2007, Refrigeration, Chapter 9) give a model for the thermal properties of a food with known component groups, dividing them in 6 categories: Water, Ice, Proteins, Carbohydrates, Fats and Ashes. Each component group is assumed to have a constant behavior, indistinctively of its internal composition. Specially for the latter four classes, which have several different substances that can be classified in each group, it might be a misleading assumption.

Although they may not behave exactly as the model predicts, the approximation was found to be the most general and reliable among the options available. Since the food composition is widely available in the literature, using the model provided by ASHRAE (2007) gives the algorithm great versatility. For example, the Brazilian university UNICAMP has compiled the Brazilian Table of Foods Composition (2011), which has been used as a data source for the experimental analysis developed in this work.

The ASHRAE model gives the thermal properties of each food component group as a continuous function of temperature. It relies on another variable, called the “initial freezing temperature”, to calculate the amount of water that has been turned into ice, given a sub-freezing temperature. Based on the ice quantity and the remaining water amount, it will calculate the properties of the food accordingly.

The graphs shown in Fig. 1 demonstrate how the model behaves for a sample product (hamburger). The sample consists of 66.3% of water, 19.7% of proteins, 11.4% of fats, 0% of carbohydrates and 2.6% of ashes. Also, its initial freezing point is -1.9ºC.

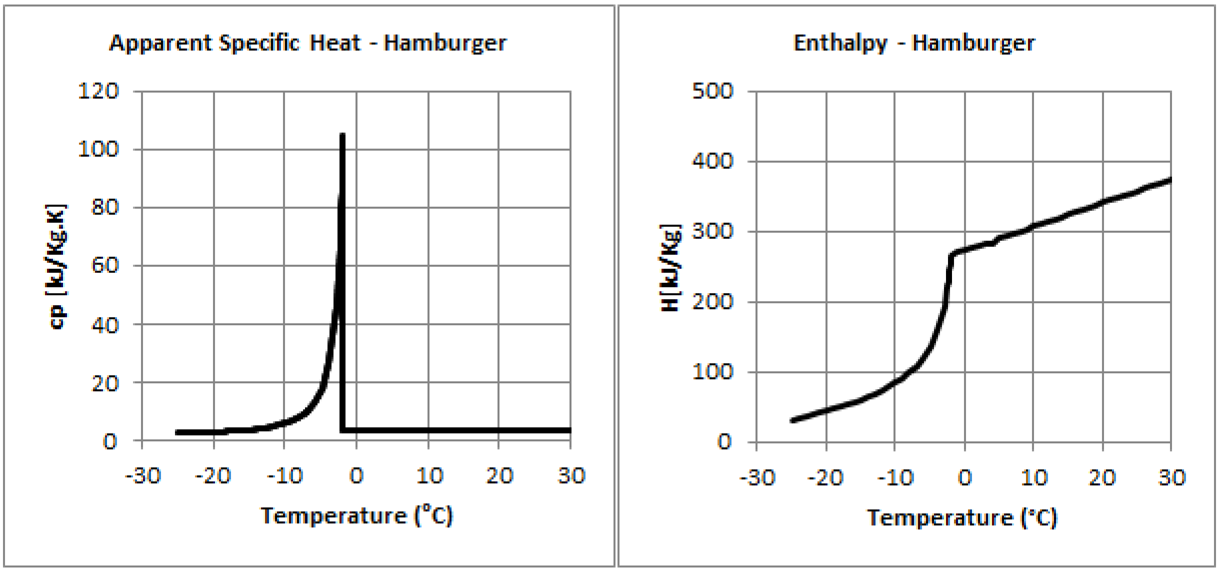

Figure 1 – Thermal property sample curves generated with ASHRAE’s methodology

Figure 1 shows that the apparent specific heat is almost constant in the unfrozen product, but when the initial freezing point is reached, it steeply jumps to a high value, about 30 times larger than the former specific heat. In the enthalpy curve, it’s clear that this discontinuity in the specific heat is reflected as a change in direction (or derivative), as is expected, given that the specific heat is the derivative of the enthalpy in relation with the temperature. These graphs shown in Fig. 1 match the geometries and trends found in experimental data, for example the curves shown in Pham et. al. (1994).

3. EXPERIMENTAL SETUP

In order to produce experimental data to validate the numerical model, an experimental pilot-scale freezing tunnel has been built. Its parts are shown in Fig. 2, and it basically consists of an insulated box with a finned evaporator, a centrifugal fan and a test section. In the test section, the product is placed along with the temperature sensors. Right after the test section, an anemometer was installed to measure the average air velocity, in order to calculate the convection coefficient.

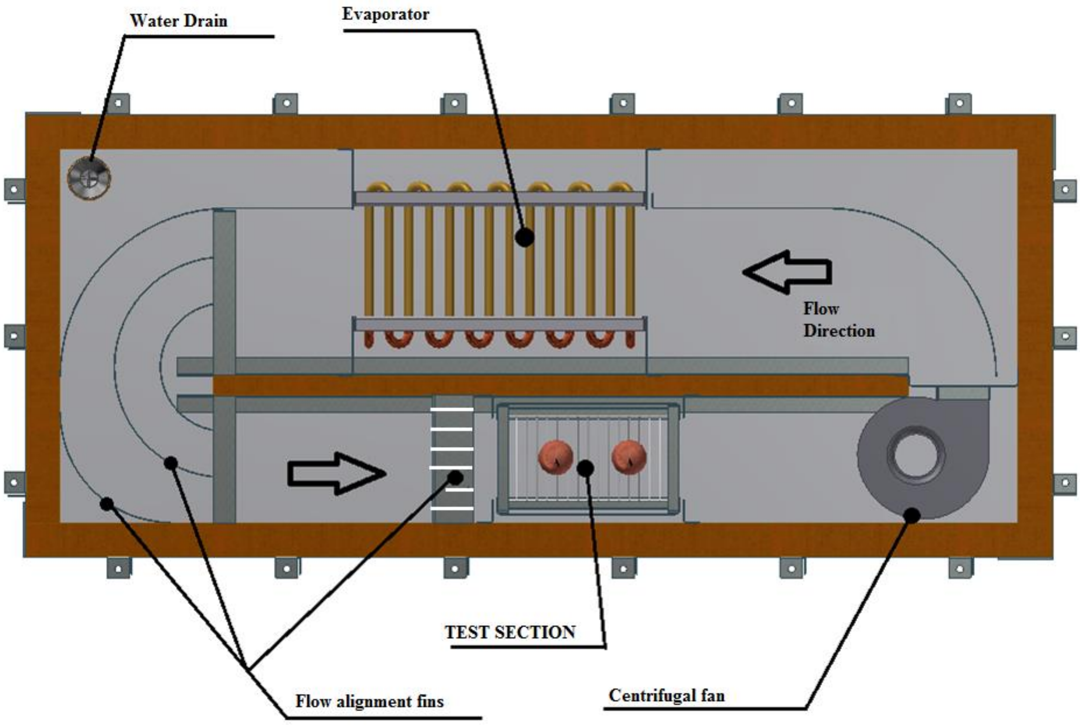

Figure 2 – Experimental freezing tunnel parts

Forty different experiments were carried out with varying parameters. The parameters and the tested range is shown in Tab. 1, below. The conditions tested try to reproduce the usual industrial conditions found in a real IQF spiral freezer.

Table 1 – Test conditions and parameter ranges

Parameter	**Tested Conditions**
Product Type	Prato Cheese, Meatballs, Sausages, Potatoes
Product Geometry	Thin Slab, Long Cylinder, Sphere
Characteristic Dimension (Diameter or Thickness)	12 mm to 60 mm
Surface Conditions	Free Surface (Conveys mass and heat) Wrapped Tinfoil (Conveys only heat)
Air Speed	2,1 m/s to 4,2 m/s
Air Temperature	-28 ºC to -33 ºC
Sensor Position	Varying from center to surface

4. RESULTS AND DISCUSSION

4.1 Data processing procedure

The data gathered from each experiment was a set of temperature measurements, collected from the beginning of the experiment until the product reached approximately -20.ºC, both for air temperature and inside temperature. Every five seconds, a temperature measurement was registered. This set of measurements was plotted into a curve of temperature versus time. Afterwards, the temperature set was loaded in the Solver, along with the experimental parameters described on Tab. 1.

The Solver is a program developed inside a Microsoft Excel Workbook. This platform was mainly chosen because of its large availability in any industry, without needing special software licenses. It runs the algorithm described in Section 2, based on product and process features inputted by the user (most of them are listed in Tab. 1), and plots a curve that represents the expected heat transfer curve for that product, based on the thermophysical properties model given by ASHRAE. The Solver allows the user to load an experimental curve and compares them giving the calculated R squared.

The Solver also allows one to modify the convection coefficient h_{used} to run the calculations, by multiplying it to a modifying variable, called $h_{Multiplier}$. The relationship between the variables is shown in Eq. 19:

$$h_{used} = h_{Multiplier} \cdot h_{correlation} \quad (19)$$

Where $h_{correlation}$ is the convection coefficient that is calculated by using the classic correlations, listed in Eq. 11 to 14. This multiplier variable has been created to enable data analysis, because in most cases it was found that the curve fitting quality would be very high, if the convection coefficient were changed. Another way to interpret this variable $h_{Multiplier}$ is as a measurement of how far or close the experimental convection coefficient was in relation to the theoretical coefficient. Since it is known that the convection coefficients calculated using Eq. 11 to 14 are prone to uncertainties of 30% (Incropera & DeWitt, 2006), changing the convection coefficient to fit the curve was the approach that resulted in less impact in the data analysis.

4.2 Discussion of the results

Two samples of the graphs and the curves that the Solver generates are shown in Fig. 3. As it can be seen, the blue (simulation) curves fit very well in the experimental (black, dashed) curves. The red curves only show the simulated surface temperature, for reference. The R^2 coefficients are very high, indicating a good fit. Most experimental data had fittings of this quality.

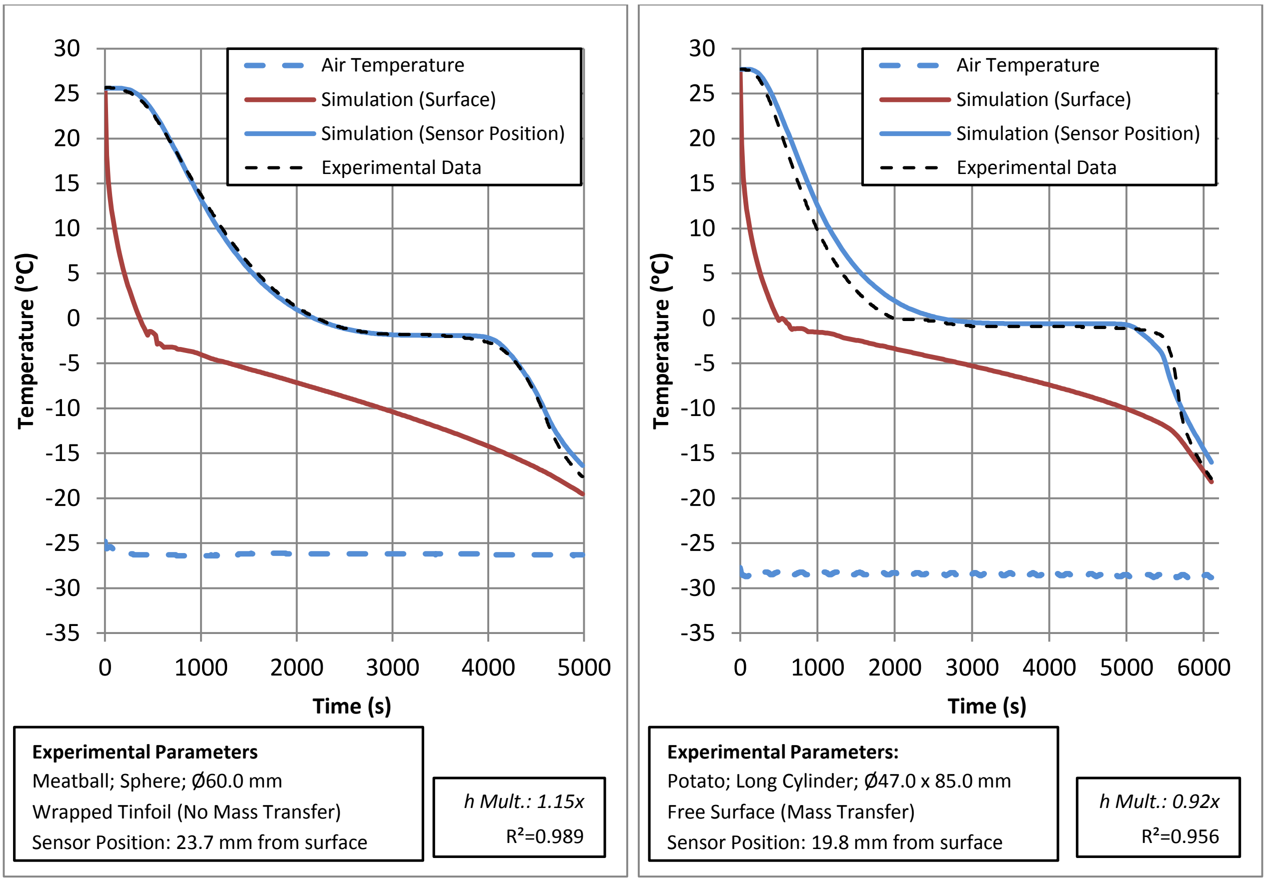

Figure 3 – Sample graphs of experimental data gathered and curve fittings

The vast majority of the experiments gave a good fit (38/40 experiments with $R^2 \geq 0.9$), and also a good part of the experiments had an acceptable prediction for h (26/40) without employing the $h_{Multiplier}$.

4.3 Comparison of the results with existing correlations

To get a better grasp on whether or not the predictions of the presented algorithm were an improvement in relation to simple correlations existing in the literature, the simulated data was compared with two different, classic correlations that were designed to forecast the freezing time of a food. The data points are plotted in Fig. 4.

The first correlation (shown as blue triangles in Fig. 4) is Planck's correlation, which dates from 1944, and can be found in Stoecker (2004). The second correlation (shown as red circles) is designed by Pham (1984), apud Fricke &

Becker (2002). They were compared with results from the solver with $h_{Multiplier} = 1$, which means that no adjustment has been made (black squares).

For each experiment, the freezing temperature (or final temperature) was fixed to be -12 ºC, mainly because of its relevance in food freezing processes throughout Brazilian food industry. Therefore, the experimental times plotted in Fig. 4 relate to the time needed to freeze the product from the starting variable temperature to -12 ºC.

Observing Fig. 4, it can be seen that Pham's correlation mostly underestimates the freezing times, while both Pham and the Solver seem to overestimate the freezing times. It also can be seen that Pham's correlation gets higher error levels. When the Solver knows the correct convection coefficient, it always gets a good prediction, within a ±5% error margin.

The average error for Pham's predictions was of 50.7%, while Planck's average was 38.8%. The Solver performed with an average error of 28.9%. It is expected that, with the correction of the convection coefficient, the average error will drop much more, achieving errors in the order of 2%, well below those achieved using the usual correlations.

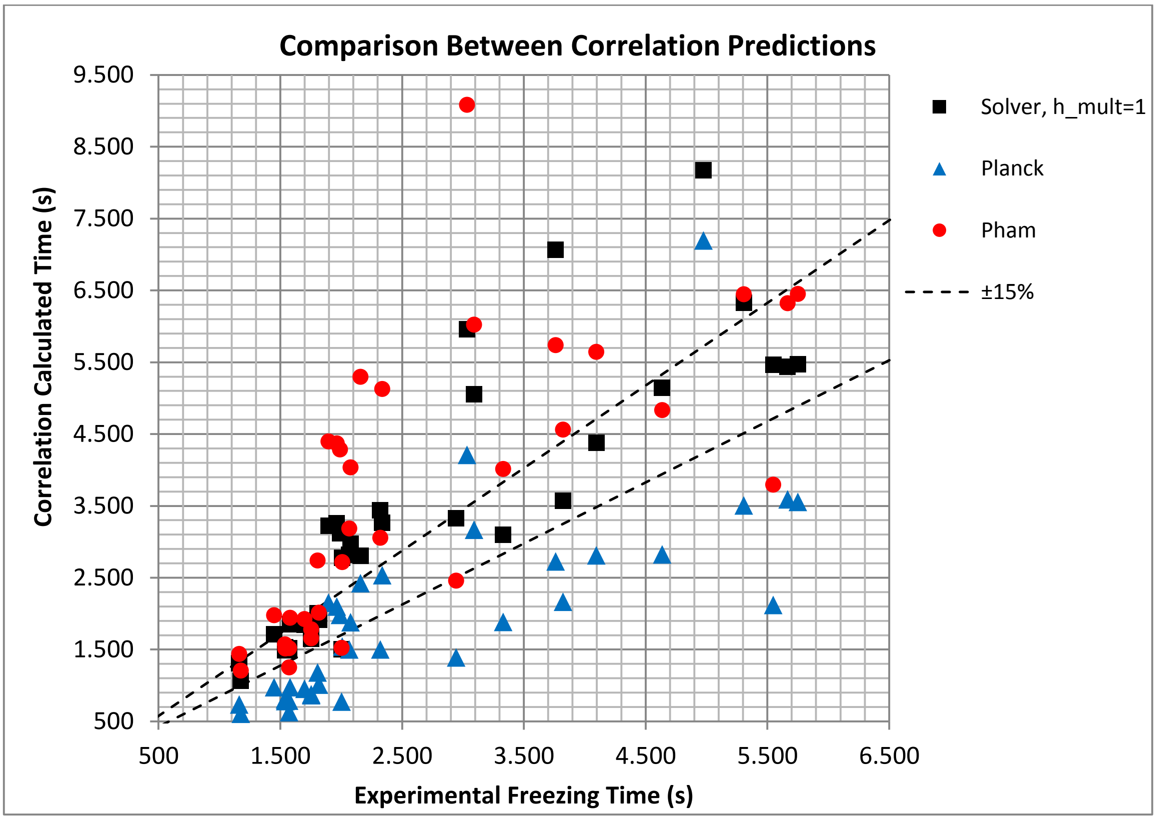

Figure 4 – Correlation predictions plotted versus experimental freezing time

5. FINAL REMARKS

The results presented in this work show that it is possible to predict with reasonable accuracy the freezing time of food products using simple numerical algorithms. It also shows that the convection coefficient has an important influence on the food freezing time, and even though there are correlations already available in the literature to predict its value, their applicability to experiments or industrial processes that do not strictly reproduce the original experimental conditions used to generate their values might be limited.

6. ACKNOWLEDGEMENTS

The authors acknowledge CNPq and UNISINOS for funding. F. Zinani is a grant holder of CNPq.

7. REFERENCES

ASHRAE. (2007). ASHRAE Handbooks. In *Refrigeration.* ASHRAE Standards.
Chapra, S. C., & Canale, R. P. (2010). *Numerical Methods for Engineers* (6th ed.). McGraw-Hill.
Fricke, B. A., & Becker, B. R. (2002). *Food Freezing Times and Heat Transfer Coefficients.* Retrieved Janeiro 31, 2015, from http://b.web.umkc.edu/beckerb/publications/conferences/freezing_times.pdf
Incropera, F., & DeWitt, D. P. (2006). *Fundamentals of Heat and Mass Transfer* (7th ed.). Wiley.

Ozisik, N. (1994). *Finite Difference Methods in Heat Transfer.* CRC Press.
Pham, Q. T., Wee, H. T., Kemp, R. M., & Lindsay, D. T. (1994). Determination of Enthalpy of Foods by an Adiabatic Calorimeter. *Journal of Food Engineering*, pp. 137-156.
Stoecker, W. F. (2004). *Industrial Refrigeration Handbook.* McGraw-Hill.
Stoecker, W. F., & Jones, J. W. (1983). *Refrigeration and Air Conditioning.* McGraw-Hill.
UNICAMP. (2011). *Tabela Brasileira de Composição de Alimentos – TACO.* Retrieved Janeiro 26, 2015, from NEPA - Unicamp: http://www.unicamp.br/nepa/taco/contar/taco_4_edicao_ampliada_e_revisada.pdf?arquivo=taco_4_versao_ampliada_e_revisada.pdf

8. RESPONSIBILITY NOTICE

The authors are the only responsibles for the printed material included in this paper.